BOSTER
antibody and ELISA experts

BOSTER BIOLOGICAL TECHNOLOGY
3942 B Valley Ave, Pleasanton, CA 94566
888-466-3604 | support@bosterbio.com | www.bosterbio.com

Anti-HIF-1-alpha/HIF1A Antibody Picoband®

Catalog Number: PB9253

About HIF1A

HIF-1alpha (Hypoxia-inducible factor 1alpha, HIF1A) is a transcription factor that mediates cellular and systemic homeostatic responses to reduced O2 availability in mammals, including angiogenesis, erythropoiesis and glycolysis. This gene was mapped to 14q21-q24. HIF-1alpha transactivate genes required for energy metabolism and tissue perfusion and is necessary for embryonic development and tumor explant growth. HIF-1alpha is over expressed during carcinogenesis, myocardial infarction and wound healing. It is crucial for the cellular response to hypoxia and is frequently over expressed in human cancers, resulting in the activation of genes essential for cell survival. HIF-1alpha regulates the survival and function in the inflammatory microenvironment directly. It is a transcription factor that plays a pivotal role in cellular adaptation to changes in oxygen availability.

Overview

Product Name	Anti-HIF-1-alpha/HIF1A Antibody Picoband®
Reactive Species	Human, Mouse, Rat
Description	Boster Bio Anti-HIF-1-alpha/HIF1A Antibody Picoband® catalog # PB9253. Tested in IHC, WB applications. This antibody reacts with Human, Mouse, Rat. The brand Picoband indicates this is a premium antibody that guarantees superior quality, high affinity, and strong signals with minimal background in Western blot applications. Only our best-performing antibodies are designated as Picoband, ensuring unmatched performance.
Application	IHC, WB
Clonality	Polyclonal
Formulation	Each vial contains antibody formulated with stabilizing components, 0.9 mg NaCl, 0.2 mg Na2HPO4, and 0.05 mg NaN3. *This antibody is supplied in a stabilized formulation. Compatibility with conjugation reactions depends on the chemistry of the conjugation method used. For conjugation methods that are not compatible with the stabilizing components present in this formulation, a carrier-free antibody format is required.
Storage Instructions	Store at -20˚C for one year from date of receipt. After reconstitution, at 4˚C for one month. It can also be aliquotted and stored frozen at -20˚C for six months. Avoid repeated freeze-thaw cycles.
Host	Rabbit
Uniprot ID	Q16665

Technical Details

Immunogen	A synthetic peptide corresponding to a sequence at the C-terminal of human HIF-1-alpha, different from the related mouse and rat sequences by three amino acids.
Recommended Detection Systems	Boster recommends Enhanced Chemiluminescent Kit with anti-Rabbit IgG (EK1002) for Western

BOSTER BIOLOGICAL TECHNOLOGY
3942 B Valley Ave, Pleasanton, CA 94566
888-466-3604 | support@bosterbio.com | www.bosterbio.com

	blot, and HRP Conjugated anti-Rabbit IgG Super Vision Assay Kit (SV0002-1) for IHC(P).
Cross Reactivity	No cross-reactivity with other proteins
Isotype	Rabbit IgG
Form	Lyophilized
Concentration	Adding 0.2 ml of distilled water will yield a concentration of 500 ug/ml.
Purification	Immunogen affinity purified.
Suggested Dilutions	Immunohistochemistry (Paraffin-embedded Section), 0.5-1ug/ml, Human, Mouse, Rat Western blot, 0.1-0.5ug/ml, Human, Mouse

BOSTER BIOLOGICAL TECHNOLOGY
3942 B Valley Ave, Pleasanton, CA 94566
888-466-3604 | support@bosterbio.com | www.bosterbio.com

Anti-HIF-1-alpha/HIF1A Antibody Picoband® (PB9253) Images

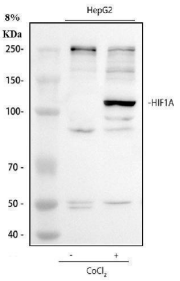

Western blot analysis of HIF 1 alpha using anti-HIF 1 alpha antibody (PB9253). Electrophoresis was performed on a 8% SDS-PAGE gel at 80V (Stacking gel) / 120V (Resolving gel) for 2 hours. The sample well of each lane was loaded with 30 ug of sample under reducing conditions. Lane 1: Untreated human HepG2 whole cell lysates, Lane 2: Cobalt Chloride treated human HepG2 whole cell lysates. After electrophoresis, proteins were transferred to a nitrocellulose membrane at 150 mA for 50-90 minutes. Blocked the membrane with 5% non-fat milk/TBS for 1.5 hour at RT. The membrane was incubated with rabbit anti-HIF 1 alpha antigen affinity purified polyclonal antibody (PB9253) at 0.5 ug/mL overnight at 4°C, then washed with TBS-0.1%Tween 3 times with 5 minutes each and probed with a goat anti-rabbit IgG-HRP secondary antibody (Catalog # BA1054) at a dilution of 1:5000 for 1.5 hour at RT. The signal is developed using an ECL Plus Western Blotting Substrate (Catalog # AR1196-200) with Tanon 5200 system. A specific band was detected for HIF 1 alpha at approximately 120 kDa. The expected band size for HIF 1 alpha is at 93 kDa.

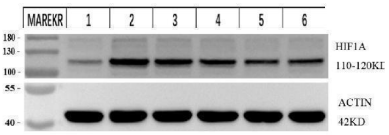

Western blot analysis of HIF1A using anti-HIF1A antibody (PB9253). Electrophoresis was performed on a 5-20% SDS-PAGE gel at 70V (Stacking gel) / 90V (Resolving gel) for 2-3 hours. The sample well of each lane was loaded with 30 ug of sample under reducing conditions. Lane 1: mouse 4T1 whole cell lysates, Lane 2: LPS-stimulated mouse 4T1 whole cell lysates, Lane 3: Low-dose drug mouse 4T1 whole cell lysates, Lane 4: Medium-dose drug mouse 4T1 whole cell lysates, Lane 5: High-dose drug mouse 4T1 whole cell lysates, Lane 6: Positive control drug mouse 4T1 whole cell lysates. After electrophoresis, proteins were transferred to a nitrocellulose membrane at 150 mA for 50-90 minutes. Blocked the membrane with 5% non-fat milk/TBS for 1 hour at RT. The membrane was incubated with rabbit anti-HIF1A antigen affinity purified monoclonal antibody (Catalog # PB9253) at 1:2500 overnight at 4°C, then washed with TBS-0.1%Tween 3 times with 5 minutes each and probed with a goat anti-rabbit IgG-HRP secondary antibody at a dilution of 1:10000 for 1 hour at RT. The signal is developed using an Enhanced Chemiluminescent detection (ECL) kit with ChemiDoc MP system. A specific band was detected for HIF1A at approximately 110-120 kDa. The expected band size for HIF1A is at 120kDa.

IHC analysis of HIF 1 alpha using anti-HIF 1 alpha antibody (PB9253). HIF 1 alpha was detected in paraffin-embedded section of mouse intestine tissue. Heat mediated antigen retrieval was performed in citrate buffer (pH6, epitope retrieval solution) for 20 mins. The tissue section was blocked with 10% goat serum. The tissue section was then incubated with 1ug/ml rabbit anti-HIF 1 alpha Antibody (PB9253) overnight at 4°C. Biotinylated goat anti-rabbit IgG

BOSTER BIOLOGICAL TECHNOLOGY
3942 B Valley Ave, Pleasanton, CA 94566
888-466-3604 | support@bosterbio.com | www.bosterbio.com

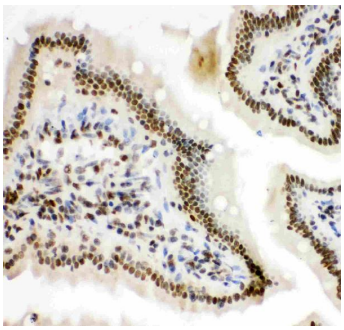

was used as secondary antibody and incubated for 30 minutes at 37°C. The tissue section was developed using Strepavidin-Biotin-Complex (SABC)(Catalog # SA1022) with DAB as the chromogen.

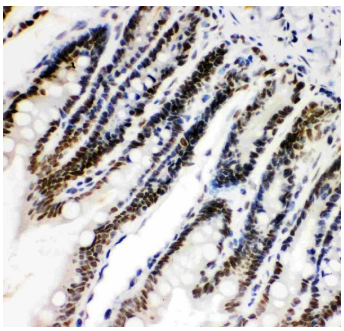

IHC analysis of HIF 1 alpha using anti-HIF 1 alpha antibody (PB9253). HIF 1 alpha was detected in paraffin-embedded section of rat intestine tissue. Heat mediated antigen retrieval was performed in citrate buffer (pH6, epitope retrieval solution) for 20 mins. The tissue section was blocked with 10% goat serum. The tissue section was then incubated with 1ug/ml rabbit anti-HIF 1 alpha Antibody (PB9253) overnight at 4°C. Biotinylated goat anti-rabbit IgG was used as secondary antibody and incubated for 30 minutes at 37°C. The tissue section was developed using Strepavidin-Biotin-Complex (SABC)(Catalog # SA1022) with DAB as the chromogen.

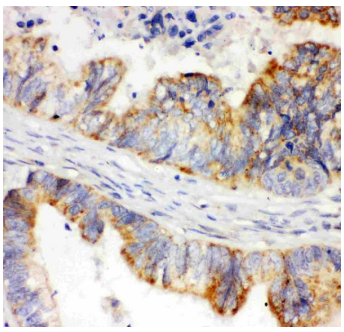

IHC analysis of HIF 1 alpha using anti-HIF 1 alpha antibody (PB9253). HIF 1 alpha was detected in paraffin-embedded section of human intestinal cancer tissue. Heat mediated antigen retrieval was performed in citrate buffer (pH6, epitope retrieval solution) for 20 mins. The tissue section was blocked with 10% goat serum. The tissue section was then incubated with 1ug/ml rabbit anti-HIF 1 alpha Antibody (PB9253) overnight at 4°C. Biotinylated goat anti-rabbit IgG was used as secondary antibody and incubated for 30 minutes at 37°C. The tissue section was developed using Strepavidin-Biotin-Complex (SABC)(Catalog # SA1022) with DAB as the chromogen.

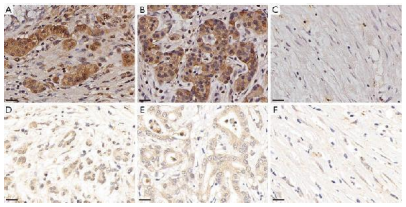

HIF-1alpha expression was analyzed by immunohistochemistry. Results of a 61-year-old male patient who underwent NAC and surgery treatment for PDAC, and had a CAP score of 2, which indicated that he was a responder. HIF-1alpha was highly expressed in the (A) nucleus (weighted score 12), (B) cytoplasm (weighted score 12), and (C) stroma (weighted score 4); results of a 30-year-old male patient who underwent NAC and surgery treatment for PDAC, and had a CAP score of 3, which indicated that he was a non-responder. HIF-1alpha was lowly expressed in the (D) nucleus (weighted score 4), (E) cytoplasm (weighted score 4), and (F) stroma (weighted score 4). 40×; scale bar =20 μm. NAC, neoadjuvant chemotherapy; PDAC, pancreatic ductal adenocarcinoma; CAP, the College of American Pathologists; HIF-1alpha, hypoxia-inducible factor-1-alpha. PMID: 39839013

Histological and immunohistochemical images of the rat

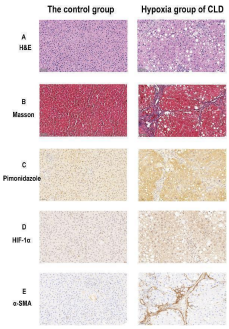

livers of the control group and hypoxia group of CLD. (A) H&E staining images (× 40) of the control and hypoxia group of CLD. (B) Masson staining images (× 40) of the control group and hypoxia group of CLD. (C) Pimonidazole Immunohistochemical staining images (× 40) of control and hypoxia group of CLD. (D) HIF-1alpha Immunohistochemical staining images (× 40) of control and hypoxia group of CLD. (E) alpha-SMA Immunohistochemical staining images (× 40) of control and hypoxia group of CLD.Index in PubMed under a CC BY license. PMID: 39906347

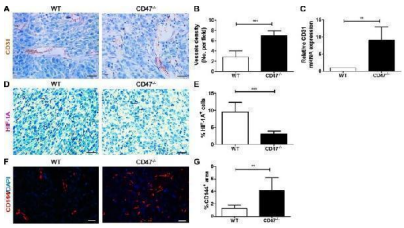

Tumors from CD47-deficient mice exhibited improved tumor angiogenesis and vascular integrity compared to those from WT mice. Tumors were surgically removed from WT or CD47 −/− mice 11 days after tumor cell injection for the following analyses (n = 4 per group). (A) Representative images of CD31 staining (black arrow) of tumor sections (Scale bar, 20 um). (B) The microvessel density (MVD) quantified by counting positive cells in six randomly selected fields (400×) using Image Pro Plus 6.0 software. (C) CD31 mRNA levels in tumors quantified by real-time qPCR. (D) Representative images of HIF-1A staining (pink) of tumor sections (Scale bar, 20 um). (E) Percentages of HIF-1A + cells in tumors quantified by counting positive cells in six randomly selected fields (400×) using Image Pro Plus 6.0 software. (F) Representative images of CD144 staining (red) of tumor sections (Scale bar, 20 um). (G) Percentages of CD144 + area in tumors quantified using Image Pro Plus 6.0 software. Data are mean ± SDs. ** P < 0.01, *** P < 0.001.Index in PubMed under a CC BY license. PMID: 27283989

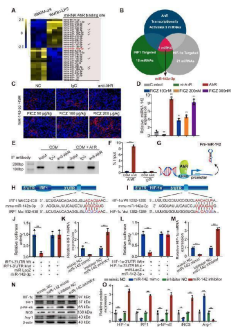

AhR transcriptionally activates miR-142a to inhibit IRF1 and HIF-1alpha expression. (A) The top 30 miRNAs in BMDMs that are regulated by LPS are arranged in a miRNA array heatmap. In addition, miRNAs predicted to be under the transcriptional control of AhR (according to analysis with the JASPAR database) are noted. (B) Venn diagram analyses were performed to identify miRNAs that can both target IRF1 and HIF-1alpha and that are under the transcriptional control of AhR. (C) Renal expression of mmu-miR-142a-3p in mice (n = 6) with CaOx nephrocalcinosis following treatment with an AhR neutralizing antibody or FICZ treatment was assessed via FISH (200×; scale bar: 20 μm). (D) qRT-PCR was performed to measure mmu-miR-142a-3p expression in BMDMs using U6 RNA as a normalization control. (E, F) ChIP assays and ChIP qPCR analysis showed that AhR bound to the miR-142a promoter in BMDMs treated with the AhR overexpression plasmid. (G) A schematic model showed that AhR directly binds to the miR-142a promoter and activates its transcription. (H, I) WT and mutated miR-142a targeting sequences in the IRF1 and HIF-1alpha 3'-UTR regions that were used to construct luciferase reporters, with reporters bearing these IRF1 (J) or HIF-1alpha (L) 3'-UTR sequences co-transfected along with miR-142a mimic (100 nM). IRF1 (K) and HIF-1alpha (M) mRNA levels were detected via qRT-PCR in BMDMs following miR-142a mimic or inhibitor transfection. Western blotting (N, O) analysis enabled the detection of

BOSTER BIOLOGICAL TECHNOLOGY
3942 B Valley Ave, Pleasanton, CA 94566
888-466-3604 | support@bosterbio.com | www.bosterbio.com

IRF1 and HIF-1alpha expression while also assessing the levels of iNOS and Arg-1 to monitor the polarization state of BMDMs following miR-142a mimic or inhibitor transfection. beta-actin was employed as a normalization control. The data are shown as the means ± SD of triplicate experiments. *P < 0.05; **P < 0.01, as assessed via Student's t test (D, F) or one-way ANOVA (J-M, O). PMID: 33204326

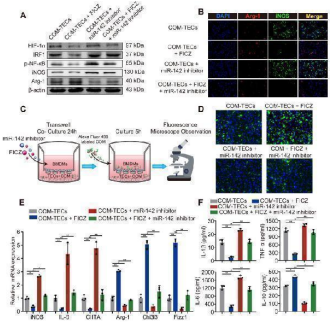

AhR activation in vitro decrease M1 macrophage polarization to inhibit kidney inflammation and injury through the AhR-miR-142a-IRF1/HIF-1alpha axis in vitro . (A) Western blotting analysis enabled the detection of AhR, HIF-1alpha, IRF1, NF-kappaB p65, iNOS, and Arg-1 expression in BMDMs. beta-actin was detected as an internal control. (B) iNOS (M1 macrophage marker, green) and Arg-1 (M2 macrophage marker, red) distributions in BMDMs were detected by immunofluorescence (200×; scale bar: 20 μm). (C) Schematic diagram of BMDMs phagocytic capacity testing. (D) Fluorescence microscopy was performed to analyse the phagocytic ability of BMDMs (200×; scale bar: 20 μm). (E) qRT-PCR analysis of iNOS, IL-6, CIITA, Arg-1, Chi3l3 and Fizz1 expression to further determine polarization state of BMDM. (F) ELISA was used to quantify cytokine levels in the co-culture media. The data are shown as the means ± SD of triplicate experiments. *P < 0.05; **P < 0.01, as assessed via one-way ANOVA (E, F). PMID: 33204326

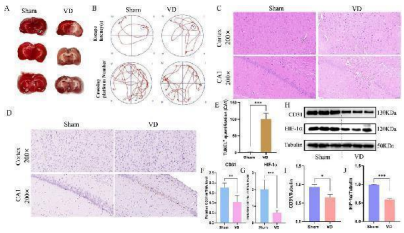

Construction of animal models and analysis of pathological damage. (A) TTC staining plots of the Sham and VD group. (B) Motion trajectory diagram. (C) Representative images stained with HE (scale bars = 50 um). (D) Representative histopathological images obtained from TUNEL staining (scale bars = 50 um), showing changes in the cortex hippocampus CA1. (E) Quantification of TUNEL+ cells in the hippocampal CA1 (n = 3). (F) Expression profile of CD31 between Sham and VD groups (qPCR). **P < 0.01. (G) Expression profile of HIF-1alpha between Sham and VD groups (qPCR; n = 6). ***P < 0.001. (H) WB strips. (I) Expression profile of CD31 between Sham and VD groups (WB). *P < 0.05. (J) Expression profile of HIF-1alpha between Sham and VD groups (WB; n = 3). ***P < 0.001. PMID: 40988927

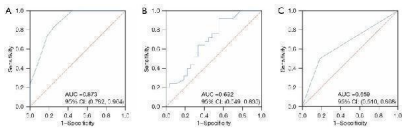

Receiver operator characteristic curves of nuclear HIF-1alpha expression (A), %ΔCA19-9 (B), and tumor differentiation (C) for predicting the post-NAC pathological response. HIF-1alpha, hypoxia-inducible factor-1alpha; NAC, neoadjuvant chemotherapy; %Δ, [(post-NAC − pre-NAC)/pre-NAC]; CA19-9, carbohydrate antigen 19-9; AUC, area under the curve; CI, confidence interval. PMID: 39839013

Effect of neohesperidin and naringin on cell viability, HIF-1alpha, Caspase3, PLIN2 in PASMCs. A – D Effects of

BOSTER BIOLOGICAL TECHNOLOGY
3942 B Valley Ave, Pleasanton, CA 94566
888-466-3604 | support@bosterbio.com | www.bosterbio.com

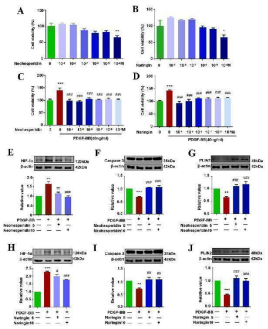

neohesperidin and naringin on PASMCs viability were observed by MTT (n = 6). E – J Expression levels of HIF-1alpha, Caspase3, PLIN2 in PASMCs were evaluated by Western Blot (n ≥ 3). * p

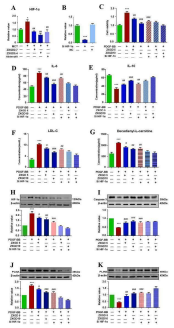

ZXGD modulated HIF-1alpha mediated pulmonary vascular remodeling. A Expression level of HIF-1alpha in lung tissue of rats was tested with PCR (n = 3). B Expression level of HIF-1alpha in PASMCs transfected with siRNA (n = 6). C Effects of ZXGD on viability of PASMCs transfected with HIF-1alpha siRNA was examined by MTT (n = 6). D – G Levels of IL-6, IL-10, LDL-C and decadienyl- l -carnitine in PASMCs transfected with HIF-1alpha siRNA. H – K Expression level of HIF-1alpha, Caspase-3, PCNA, PLIN2 in PASMCs transfected with HIF-1alpha siRNA (n ≥ 3). * p

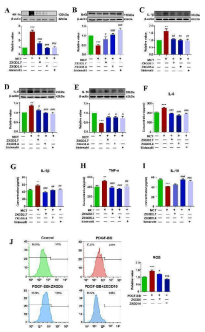

ZXGD inhibited hypoxia, oxidative stress and inflammation in rats with PH and PASMCs induced with PDGF-BB. A – E Expression of HIF-1alpha, Nrf2, IL-1beta, IL-6 and IL-10 in lung tissue of rats were detected using Western blot (n = 3 or 6). F – I Concentration of IL-6, IL-1beta, TNF-alpha and IL-10 in lung tissue of rats were examined by ELISA (n = 6). J Level of ROS in PASMCs was assessed with flow cytometry, and statistical data was obtained. ** p

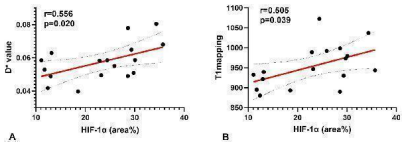

Correlations for the hypoxia score (HIF-1alpha) with the pseudo-diffusion coefficient (D*) and the T1 mapping. (A) HIF-1alpha correlated positively with the D* (r = 0.556, p = 0.020). (B) HIF-1alpha correlated positively with T1 mapping (r = 0.505, p = 0.039).Index in PubMed under a CC BY license. PMID: 39906347

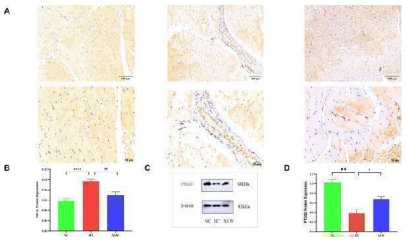

Effects of XLW on HIF1alpha and PTGS2 expressions in rat extraocular muscle tissues. (A) The immunohistochemical slice of HIF1alpha, (B) HIF1alpha immunohistochemical quantitative analysis, (C) WB of PTGS2 levels, and (D) quantification of the WB in PTGS2. ** p

Response of ZF4 cells to hypoxic stress. (A) Cell Viability was analyzed with PrestoBlue™ HS Cell Viability Regent under normoxia or hypoxia treated for 1, 2, 3 and 4 d. (B) The mRNA expression of iron absorption and storage gene in ZFL cells was quantified by real-time RT–PCR under normoxia and hypoxia for 3 days. (C) Western blot analysis of

BOSTER BIOLOGICAL TECHNOLOGY
3942 B Valley Ave, Pleasanton, CA 94566
888-466-3604 | support@bosterbio.com | www.bosterbio.com

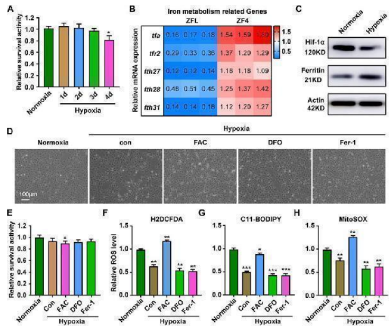

Hif-1alpha and Ferritin expression in ZF4 cells cultured under normoxia and hypoxia for 3 days. (D) The microscope analysis of morphology changes in ZF4 cells under normoxia or hypoxia treated with or without FAC (2.5 mM), DFO (10 μM) and Fer-1 (2.5 μM) for 3 days. (E) Cell Viability was analyzed with PrestoBlue™ HS Cell Viability Regent under normoxia or hypoxia treated with or without FAC (2.5 mM), DFO (10 μM) and Fer-1 (2.5 μM). (F–H) Analysis of changes in general ROS (F) , mitochondrial-derived ROS (G) and lipid peroxidation (H) levels in cells with H2DCFDA, MitoSOX and C11-BODIPY probe under normoxia and hypoxia for 3 days. Cells under hypoxic stress were rescued with FAC (2.5 mM), DFO (10 μM) and Fer-1 (2.5 μM). Normoxia was used as a control group for significance analysis. Error bars, mean ± s.d., n = 3 (biological replicates).Index in PubMed under a CC BY license. PMID: 36091397

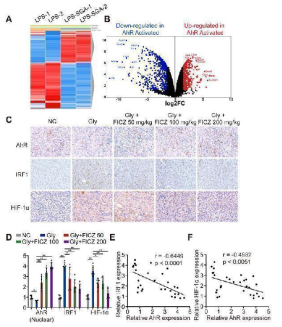

AhR significantly suppressed IRF1 and HIF-1alpha expression in a murine CaOx nephrocalcinosis model. (A) RNA-seq heatmap showing significantly altered mRNAs in SGA-treated BMDMs. (B) Volcano plots showing mRNA transcripts that were differentially expressed between LPS-treated and SGA-treated BMDMs. Significantly downregulated and upregulated mRNAs are shown in green and red, respectively, whereas genes that were not significantly changed are shown in black. (C) IHC staining for AhR, IRF1, and HIF-1alpha in the kidneys of FICZ-treated mice with CaOx nephrocalcinosis (200×; scale bar: 20 μm). (D) qRT-PCR was used to assess AhR, IRF1, and HIF-1alpha expression in kidney samples from FICZ-treated mice (n = 6) with CaOx nephrocalcinosis compared to kidney samples from model mice. (E, F) Pearson's correlation coefficient analysis (n = 30) of the expression levels of AhR and IRF1 (E) or HIF-1alpha (F). Each dot represents an individual animal. *P < 0.05; **P < 0.01, as assessed via one-way ANOVA (D).Index in PubMed under a CC BY license. PMID: 33204326

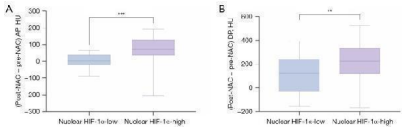

Comparison of CT values between the nuclear HIF-1alpha-high and -low expression PDAC patients following NAC. ***, P

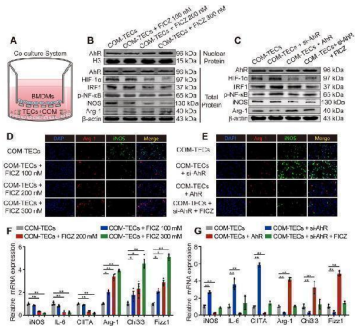

AhR suppressed IRF1 and HIF-1alpha to attenuate CaOx crystal-stimulated M1 macrophage polarization in vitro . (A) BMDMs and COM-treated TECs co-culture model. (B, C) Western blotting analysis was used to detect AhR, HIF-1alpha, IRF1, NF-kappaB p65, iNOS, and Arg-1 expression after FICZ treatment and the upregulation or downregulation of AhR in BMDMs. beta-actin served as a normalization control. (D, E) iNOS (M1 macrophage marker, green) and Arg-1 (M2 macrophage marker, red) distribution in BMDMs were detected by immunofluorescence (200×; scale bar: 20 μm). (F, G) qRT-PCR analysis of iNOS, IL-6, CIITA, Arg-1, Chi3l3 and Fizz1 expression to further determine polarization state of BMDM. The data are shown as the means ± SD of triplicate experiments. *P < 0.05; **P < 0.01, as assessed via one-way ANOVA (F, G).Index in

PubMed under a CC BY license. PMID: 33204326

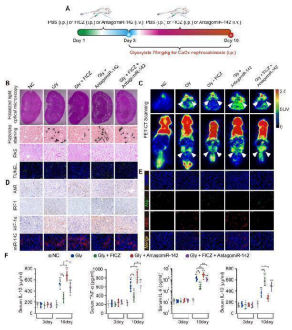

AhR activation suppressed the deposition of CaOx crystal and CaOx nephrocalcinosis-mediated kidney inflammation and injury through the AhR-miR-142a-IRF1/HIF-1alpha axis in vivo . (A) Experimental overview. (B) The deposition of renal CaOx crystal in FICZ- and/or antagomiR-142a-treated mice was assessed via polarized light optical microscopy (20×; scale bar: 500 μm). Pizzolato staining was employed as a means of detecting these CaOx crystal in corticomedullary tissue, while PAS was utilized to evaluate injury to TECs (200×; scale bar: 20 μm), and TUNEL staining was employed to assess renal TECs death (200×; scale bar: 50 μm). (C) PET-CT scanning was employed as a means of assessing renal inflammation state in CaOx nephrocalcinosis mice. (D) IHC was used to analyse AhR, IRF1, and HIF-1alpha expression, and FISH was used to detect miR-142a expression in renal tissue (200×; scale bar: 20 μm). (E) iNOS (M1 macrophage marker, red) and Arg-1 (M2 macrophage marker, green) distributions in renal tissues were detected by immunofluorescence (200×; scale bar: 50 μm). (F) On days 3 and 10, the serum pro-inflammatory IL-1beta, TNF-alpha, and IL-6 levels and the anti-inflammatory IL-10 levels were measured by ELISA. n = 6 per group. *P < 0.05; **P < 0.01, as assessed via one-way ANOVA (F).Index in PubMed under a CC BY license. PMID: 33204326

74 Publications Citing This Product

1. PubMed ID: 10.3748/wjg.v17.i14.1915, Oxidative stress and hypoxia-induced factor 1alpha expression in gastric ischemia

2. PubMed ID: 10.3109/03008200902855891, Effect of Negative Pressure on Human Bone Marrow Mesenchymal Stem Cells In Vitro

3. PubMed ID: 10.18632/oncotarget.9899, CD47 deficiency in tumor stroma promotes tumor progression by enhancing angiogenesis

Visit bosterbio.com/anti-hif-1-alpha-picoband-trade-antibody-pb9253-boster.html to see all 74 publications.